

## Supplemental Material

### Molecular Antagonism between X-Chromosome and Autosome Signals Determines Nematode Sex

Behnom Farboud<sup>1</sup>, Paola Nix<sup>1,2</sup>, Margaret M. Jow<sup>1,3</sup>, John M. Gladden<sup>1,4</sup>, and Barbara J. Meyer<sup>1,5</sup>

<sup>1</sup>Howard Hughes Medical Institute, Department of Molecular and Cell Biology, U.C. Berkeley, Berkeley, CA 94720-3204

<sup>2</sup>Current address: Department of Biology, University of Utah, Salt Lake City, UT 84112-0840

<sup>3</sup>Current address: Department of Biology, San Francisco State University, San Francisco, CA 94132

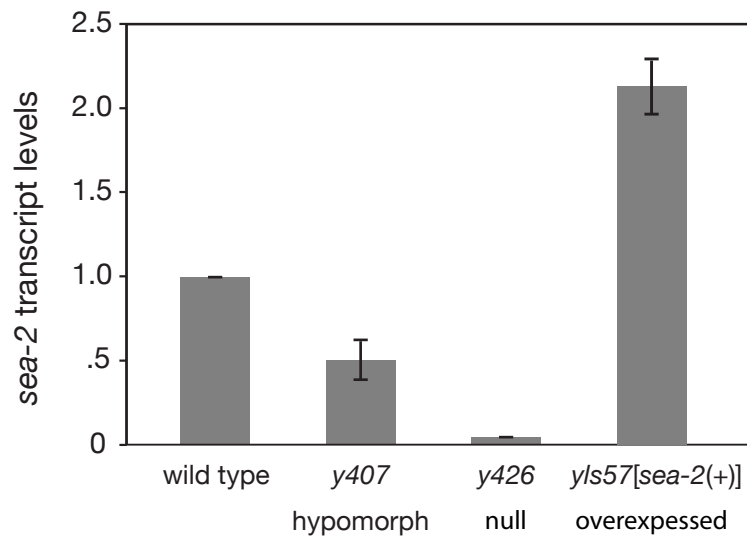
<sup>4</sup>Current address: Bioengineering & Biomass Science and Conversion Technology Department, Sandia National Laboratories, Livermore, CA 94551-0969

#### Table of Contents

Supplemental Figure 1 .....	1
<i>sea-2</i> transcript levels in different <i>sea-2</i> mutants.	
Supplemental Figure 2 .....	2
Primary amino acid sequence of SEA-2.	
Supplemental Figure 3 .....	3
<i>sea-2</i> controls sex determination and dosage compensation by acting in two separate capacities, as an activator of <i>xol-1</i> and as a regulator of dosage compensation, acting downstream of <i>xol-1</i> .	
Supplemental Figure 4 .....	5
Extra copies of <i>sea-2</i> and <i>sea-1</i> activate <i>xol-1</i> and reduce hermaphrodite viability.	
Supplemental Figure 5 .....	6
Identification of the <i>xol-1</i> transcription start site and nearby nucleosomes with and without post-translational modifications.	
Supplemental Figure 6 .....	8
SEX-1 binds directly to multiple sites in <i>xol-1</i> .	

Supplemental Figure 7 .....	10
CEH-39 binds directly to multiple sites in <i>xol-1</i> .	
Supplemental Figure 8 .....	11
SEA-1 binds directly to multiple sites in <i>xol-1</i> .	
Supplemental Figure 9 .....	14
DNase I footprinting assays identified five non-canonical T-box binding sites for SEA-1.	
Supplemental Figure 10 .....	18
SEX-1 and SEA-1 can co-occupy a fragment of <i>xol-1</i> in vitro that contains binding sites for both proteins.	
Supplemental Figure 11 .....	20
Loss of <i>tra-1</i> weakly derepress <i>xol-1</i> but does not cause significant hermaphrodite lethality at 20°C.	
Supplemental Table 1 .....	22
Mutation of XSE binding sites in a <i>xol-1</i> transgene causes increased <i>xol-1</i> transcript levels, thereby recapitulating the effect of disrupting XSE genes.	
Supplemental Materials and Methods .....	23

## Supplemental Figure 1



### ***sea-2* transcript levels in different *sea-2* mutants.**

Relative *sea-2* transcript levels in wild-type XX embryos and XX embryos carrying a *sea-2(y407)* partial loss-of-function mutation, a *sea-2(y426)* null mutation, or the integrated array *yls57* bearing multiple copies of the wild-type *sea-2* gene. Transcript levels quantified by qRT-PCR are undetectable in the *y426* mutants, consistent with the allele causing an early translation stop and mRNA degradation. Transcript levels are increased about 2-fold by the integrated *sea-2* array, consistent with modestly enhanced ASE activity.

## Supplemental Figure 2

### SEA-2

1 MEGHSSLASYSHHHPSSSHHHHPGQQSSSSSSSSSHLQDFQSPPSASHPY  
51 YHQQQPQHQQQAQQYGQATGSTNGGGQQQMTSMYGGNDYDQHLHHQNO  
101 QHQASTSTQQFHHPQRPPPPQYDQPSSSTGSSLPLHTVRYEQLPPPPSN  
151 QRTPTQQLQYPVKVVEAGGQAYAQQVQQAQQSNRSGAAGVNSALQPKPLP  
201 PLSSITSISSSAAGSSISAPSTSQPSTTSSLITSPSTSSSSMAPRKTTP  
251 NASSSSLIKRQSQDVQEQQRVDFEVARNVSQIMSKNGLKVMHEPLL TGSL  
301 PQLAPLAPLPPP KSGVYQ **CPNCNRNLANARNLQRHRQTC**GSAQHAAPQLA  
351 AMLQRSPPPCASAPPVAPPTAPSTSFQHHNSTGNLTLSYSSSSSRHQSSL  
401 YSPQLEHQDLVGNPNVMLSDGYEYKDDPMLYQGPSGLSDSIWSRDDSFHS  
451 EPPSASHDQLDMDHLGFPDPLQDPLHHLDSFDSADHRKETPRECHEPDEL  
501 MTLDPPTPPQCGSERFYGINIDDMPLSLDCDEPLMRSESASLSSSSQGRNT  
551 PAAVFT **CEACKKSVSSERSLRRHYNTCK**MFQTELAASGEETVSNSTTTTT  
601 TATTTSSKSTGNPLFT **CEHCARQLCSMSNLKRHRATC**KVAASSSSNSAAS  
651 RPPSQPSTPATAPATPMLQASQAPQPLQAPPQSPMETTATVTYTKTTVPP  
701 SVANTWNTKAQLISPKPRSQTFSEASSMTVGDALRAQQHQKMDQQI  
751 QIQFQQQQQRFQHHQQQQQAGRIPPRPPNPILNQVQNPQQVQHNQHQN  
801 QMLNPIRQPLLQSPPPPPKGLIEHKNTDLVLITSEPLAERMDAKRRSS  
851 EGLVAVTSTPLPIQLPQRSQAPAPSRQQQQPPVAYQVQFNGRPLPPMQ  
901 LPPLQNPHNQQQQHMLHQSQMNYQQVQQVQVQHVQQQNLQNQHQQ  
951 QHHQQNQQAQGNRSRSHSNVGMQEQAQRQGSPLDSIITSVPLSIEVHH  
1001 HIMKGPLEQGQSSVDSQSTAEPSPRKASQQAYI **CPECKKTYASRKNVKR**  
1051 **HRMAVH**KLTLDEILANPEQPALDPLSAVGGAGRRHTVAGLETPDSALKPA  
1101 PTKRKASEAPSAGVATKKGKAMAASVDEIQVKEEEDQKEETVGSVERQE  
1151 PPKKPVADDHKSIAIPLPPANTIMPPPPYNQASAVPLNPPRTALPPLQL  
1201 PPLQLQSESPSWASMSAPPTALIPRTPRSSEFADEEDTRAMAKIAAGLK  
1251 RSAEDWPVLAVIEGVAAEPTNGEDIDEDEILIKRLRQGGVLEDVGDVSDL  
1301 LRDVQGGVDGEPFSEDMLEKNLSTASSVGLPSLASPGEQFGYQQYSQHP  
1351 QQHPQQHPQQHPQQQQVWNPNYEFQGYMQQHPMPVVSQQFQQPLLQRP  
1401 ASQPPPARPIVKNSRRPSTTPKPPPNLT **CSGCKKILGSDYSLRRHRAGCA**  
1451 DVQQALNPEYPRPPKKAAREAQKINEAEILASMPDPQMVAAERSAAVAEA  
1501 AAAEAAVERIGALPPPSVVHEIVHQVNADRQSMKKHNKTTSPPPAQEAPP  
1551 TCAPDDPMSSSSSSSTSSASPLQGGAKPSTNQARHY **CQFPECGNFSSEW**  
1601 **NLARHTRESC**KMTTRAHSYEPTSAADKIDLIFMDKSKRRVSRFLCTVSS  
1651 LISYWLGEQGDRLELDTKWEHFQLLLDVHTLKVAITADNINLIAEQSKKY  
1701 QLEHVIRMADQFMMNTNYTTPPTHVQL

#### Primary amino acid sequence of SEA-2.

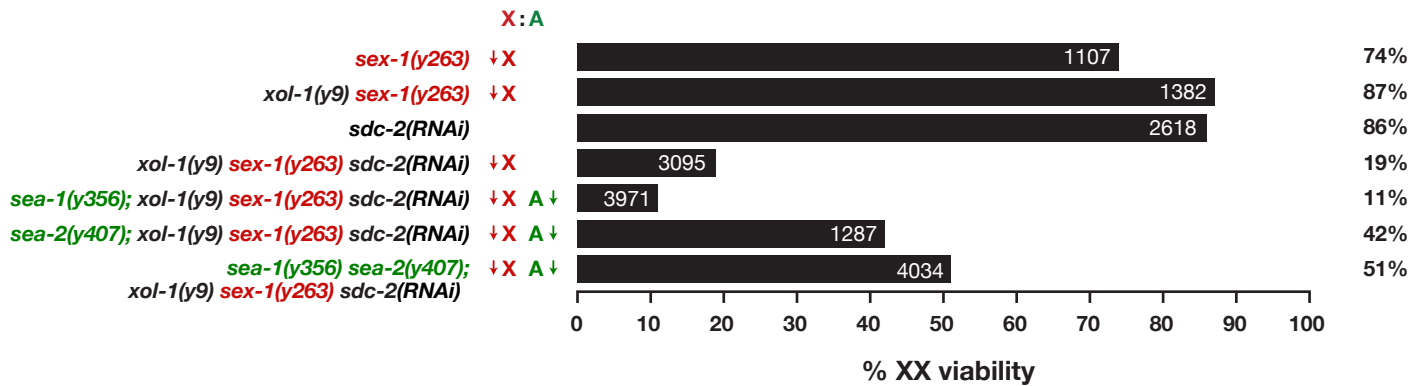
Predicted protein is encoded by the longest sea-2 transcript. Zinc finger motifs are shown in red.



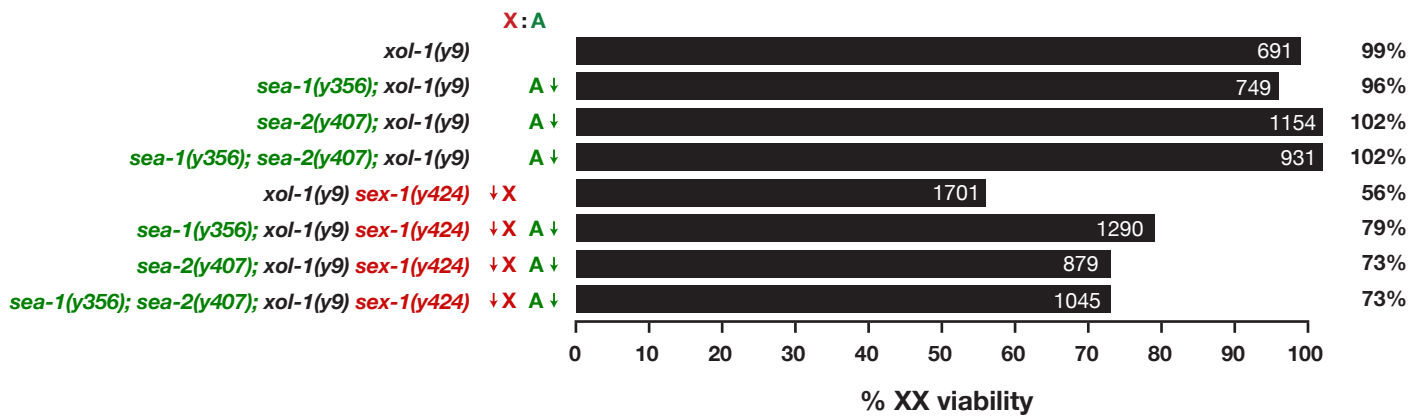
Supplemental Figure 3

**sea-2 Functions both Upstream and Downstream of *xol-1***

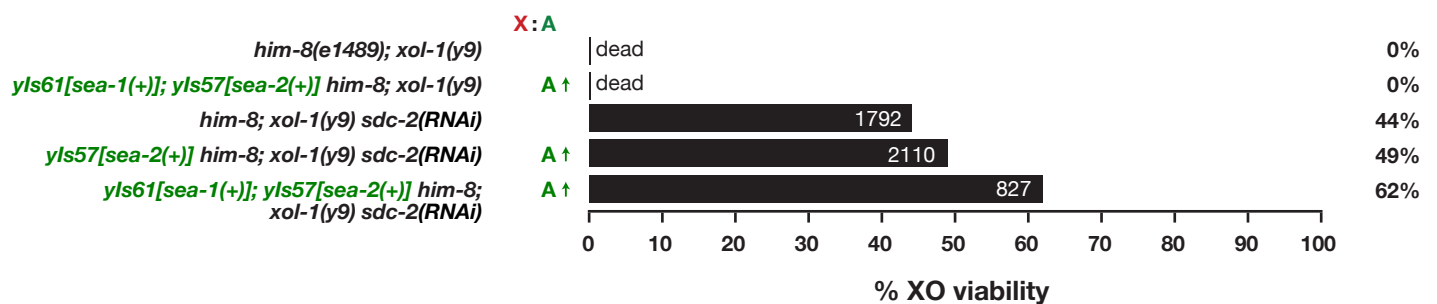
**A *sea-2* Mutations Affect Dosage Compensation Independently of the X:A Signal**



**B *sea-2* Mutations Affect the XSE-Independent Function of *sex-1***



**C Overexpression of ASEs Suppresses the Lethality of *xol-1* XO Mutants**



**Supplemental Figure 3. *sea-2* controls sex determination and dosage compensation by acting in two separate capacities, as an activator of *xol-1* and as a regulator of dosage compensation, acting downstream of *xol-1*.**

Genotype of assayed class of animals is indicated on the left, percent viability of adult XX animals is shown on the X axis, total number of embryos counted is shown on the graph (white), and effect of mutations on the X or Autosomal part of the X:A signal is indicated by arrows (decrease, down; increase, up). Viability was calculated by the formula [(no. adults) / (no. of embryos)] X 100. Details of strains and scoring are in the Materials and Methods.

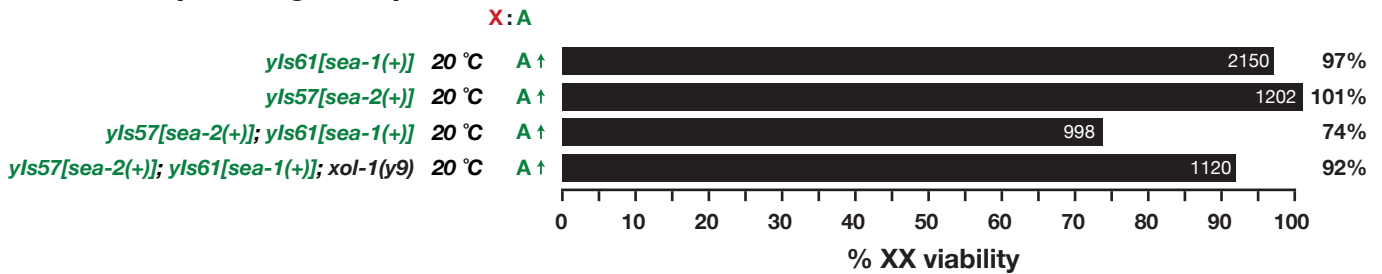
(A) A *xol-1* mutation suppresses most, but not all, of the XX lethality caused by partial disruption of the XSE *sex-1*. The residual XX lethality can be enhanced by RNAi against *sdc-2*, a dosage compensation gene that acts downstream of *xol-1* to trigger loading of the DCC onto X. *sea-2(y407)* partially suppresses the enhanced XX lethality, indicating that *sea-2* can act independently of *xol-1* to repress dosage compensation in XX animals.

(B) A *sea-2* mutation can suppress the XX lethality caused by disrupting the *xol-1*-independent activity of *sex-1*. A *xol-1* mutation partially suppresses the XX lethality caused by the *sex-1(y424)* null allele, and the *sea-2* partial loss-of-function mutation *y407* suppresses the residual XX lethality further, indicating that *sea-2* opposes the *xol-1*-independent activity of *sex-1*, either directly or indirectly.

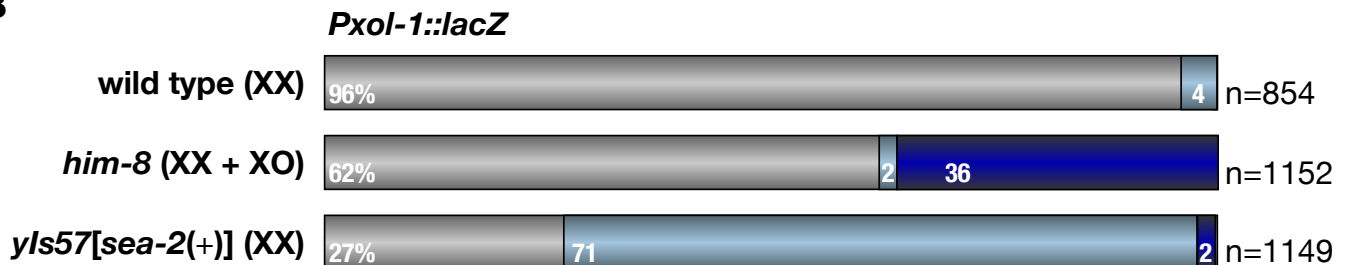
(C) Increasing the dose of *sea-1* and *sea-2* acts in concert with *sdc-2(RNAi)* to suppress the XO lethality caused by eliminating *xol-1* activity, providing further evidence that ASEs can act as negative regulators of dosage compensation, acting downstream of *xol-1*.

## Supplemental Figure 4

### A Overexpressing Multiple ASEs Kills XX Animals



### B

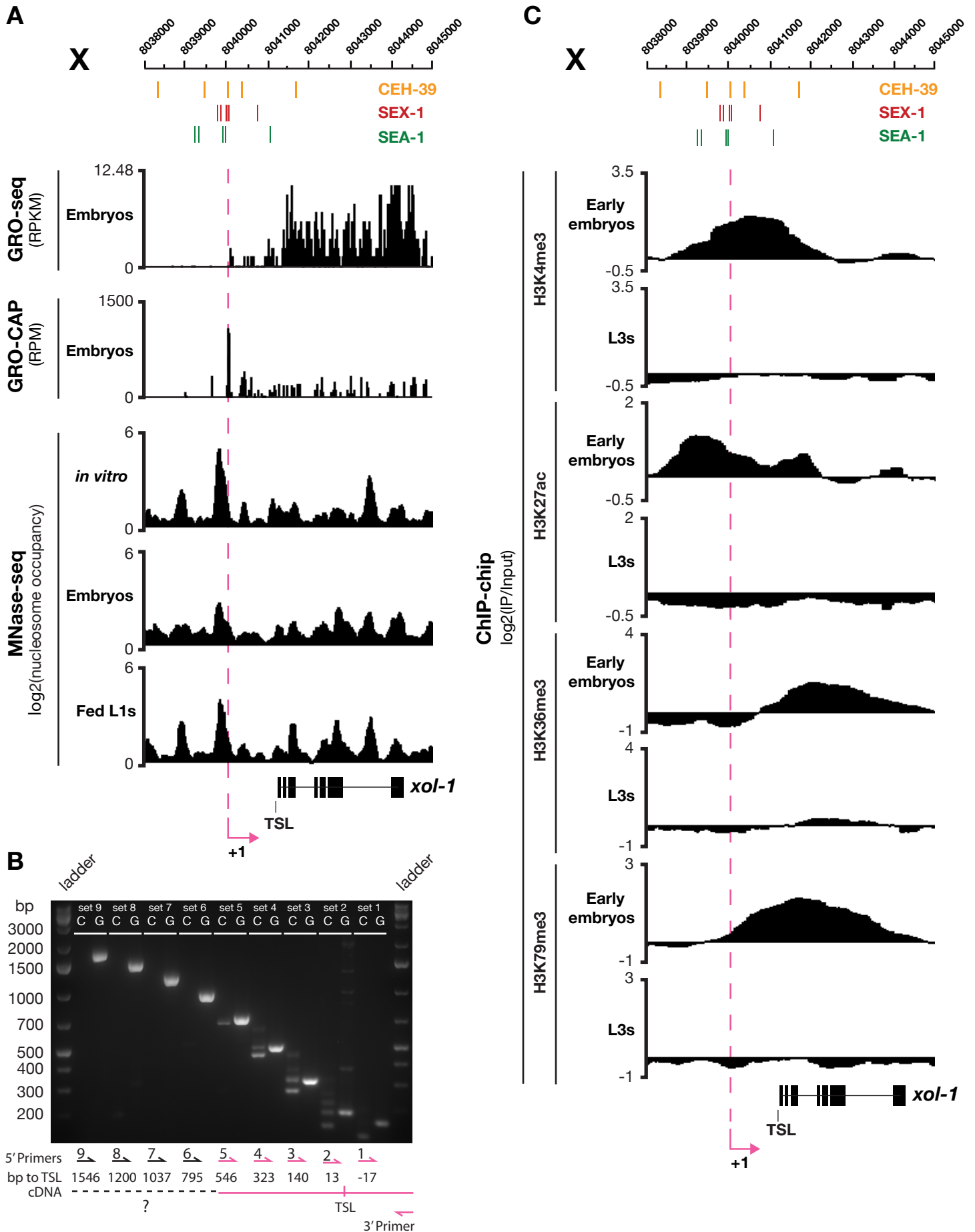


#### Extra copies of *sea-2* and *sea-1* activate *xol-1* and reduce hermaphrodite viability.

(A) Increasing the dose of both *sea-2* and *sea-1* causes a greater reduction in hermaphrodite viability than elevating the dose of either alone. The experiment was performed as in Fig. 3A, except animals were grown at 20°C instead of 25°C. An additional 22% lethality was observed at the higher temperature. Genotype of assayed animals is indicated on the left, percent viability of XX animals is shown on the X axis, total number of embryos counted is shown on the graph (white), and effect of mutations on the X or Autosomal part of the X:A signal is indicated by arrows on the left (decrease, down; increase, up). Viability was calculated by the formula [(no. adults) / (no. of embryos)] X 100. Details of strains and scoring are in the Materials and Methods.

(B) Extra copies of *sea-2* elevate *xol-1* transcription. Shown is the quantification of embryos grown at 20°C and carrying the integrated *Pxol-1::lacZ* with undetectable (gray) low (light blue) or high (dark blue)  $\beta$ -galactosidase activity when produced from hermaphrodites of genotypes listed on the left. n is the total number of embryos scored; percentage of embryos with each class of  $\beta$ -galactosidase activity is shown in white. The experiment was performed and quantified as in Fig. 4B.

Supplemental Figure 5



**Supplemental Figure 5. Identification of the *xol-1* transcription start site and nearby nucleosomes with and without post-translational modifications.**

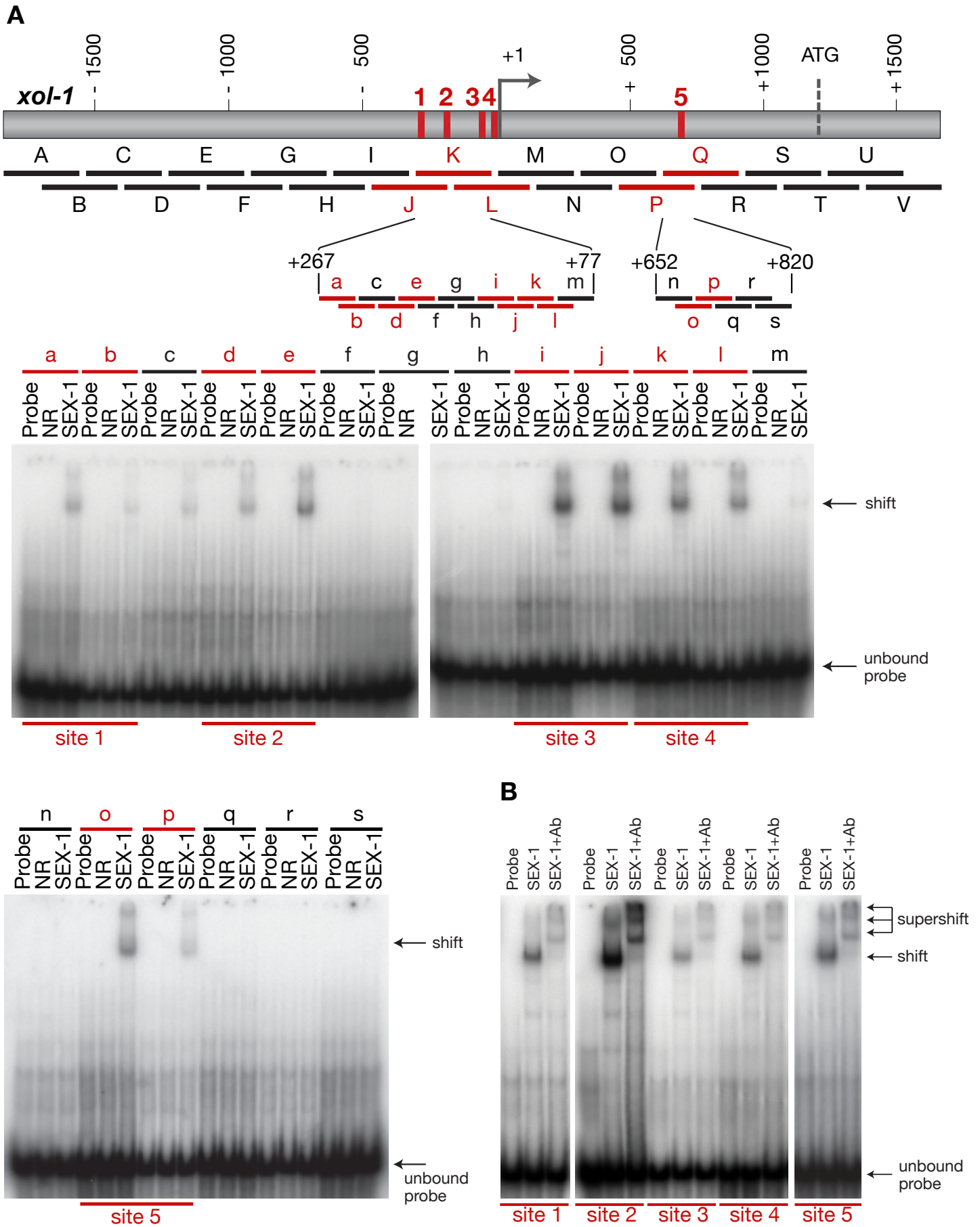
The start point of *xol-1* transcription lies 1238 bp upstream of *xol-1*'s trans-splice leader (TSL) site and is immediately downstream of a stably-positioned nucleosome. In the early embryo, when *xol-1* is active, this -1 nucleosome carries post-translational modifications typical of active transcription. Later in development, when *xol-1* is off, the modifications are absent.

(A) Global Run-On sequencing (GRO-seq) assays, performed with extracts from embryo nuclei, revealed nascent *xol-1* transcripts upstream of the amplicons identified by PCR of *xol-1* cDNA in panel B. Global Run-On sequencing coupled with enrichment for nascent RNAs with 5' CAPs (GRO-CAP) showed the location of the 5' CAP to be coincident with the 5' most GRO-seq signal, defining the transcription start site (TSS) for *xol-1* (Kruesi, W.S., Core, L.J., Waters, C.T., Lis, J.T., and Meyer, B.J., personal communication). RPKM is reads per kilobase per million mapped reads. RPM is reads per million mapped reads. Digestion of isolated chromatin with micrococcal nuclease followed by deep sequencing (MNase-seq) identified a stably-positioned -1 nucleosome directly upstream of the *xol-1* TSS in embryos, in synchronized fed L1 larvae, and in nucleosomes reconstituted *in vitro* (Preston, C, Fondufe-Mittendorf, Y., Widom, J., and Meyer, B.J., personal communication). Nucleosome occupancy is the number of raw reads per nucleotide averaged over 10 kb. The locations of CEH-39, SEX-1, and SEA-1 binding sites are shown relative to the *xol-1* TSS and gene body, nucleosomes, and genomic region on X.

(B) PCR amplification of cDNA made from early-staged embryo RNA revealed the *xol-1* TSS to be much further upstream than anticipated from the TSL location. First-strand cDNA was generated, and PCRs were then performed using a common 3' primer in the ORF and 5' primers successively further upstream from *xol-1*'s TSL. Presence of an amplicon indicated that the cDNA, and thus the TSS, is at least as far upstream as the 5' primer. Primer pairs that successfully amplified cDNA are colored magenta. bp to TSL indicates the distance from the 5' primer to the TSL and is shown below the primer designations. This approach showed the transcript to be at least 546 bp upstream of the TSL. Because trans-splicing occurs co-transcriptionally, it is rare to find the true 5' end of an mRNA in accumulated RNAs, hence the need for GRO-seq and GRO-cap. G indicates PCR amplification from genomic DNA as a control, and C indicates PCR amplification from cDNA.

(C) In the early XX embryo, *xol-1* is actively transcribed, and H3K4me3 and H3K27ac are enriched on the -1 nucleosome, and H3K36me3 and H3K79me3 are enriched in nucleosomes in the gene body, as assayed by ChIP-chip. These chromatin marks are correlated with transcription initiation or elongation, respectively. The histone marks are absent later in development, during the L3 larval stage, when *xol-1* is repressed in XX hermaphrodites. Data were obtained from the ModENCODE Consortium database (Celniker, S. E. *et al.* 2009, *Nature* 459, 927-30). For each track, the log<sub>2</sub> ratios of ChIP/Input signals are shown (z-score) for an average of two biological replicates.

Supplemental Figure 6

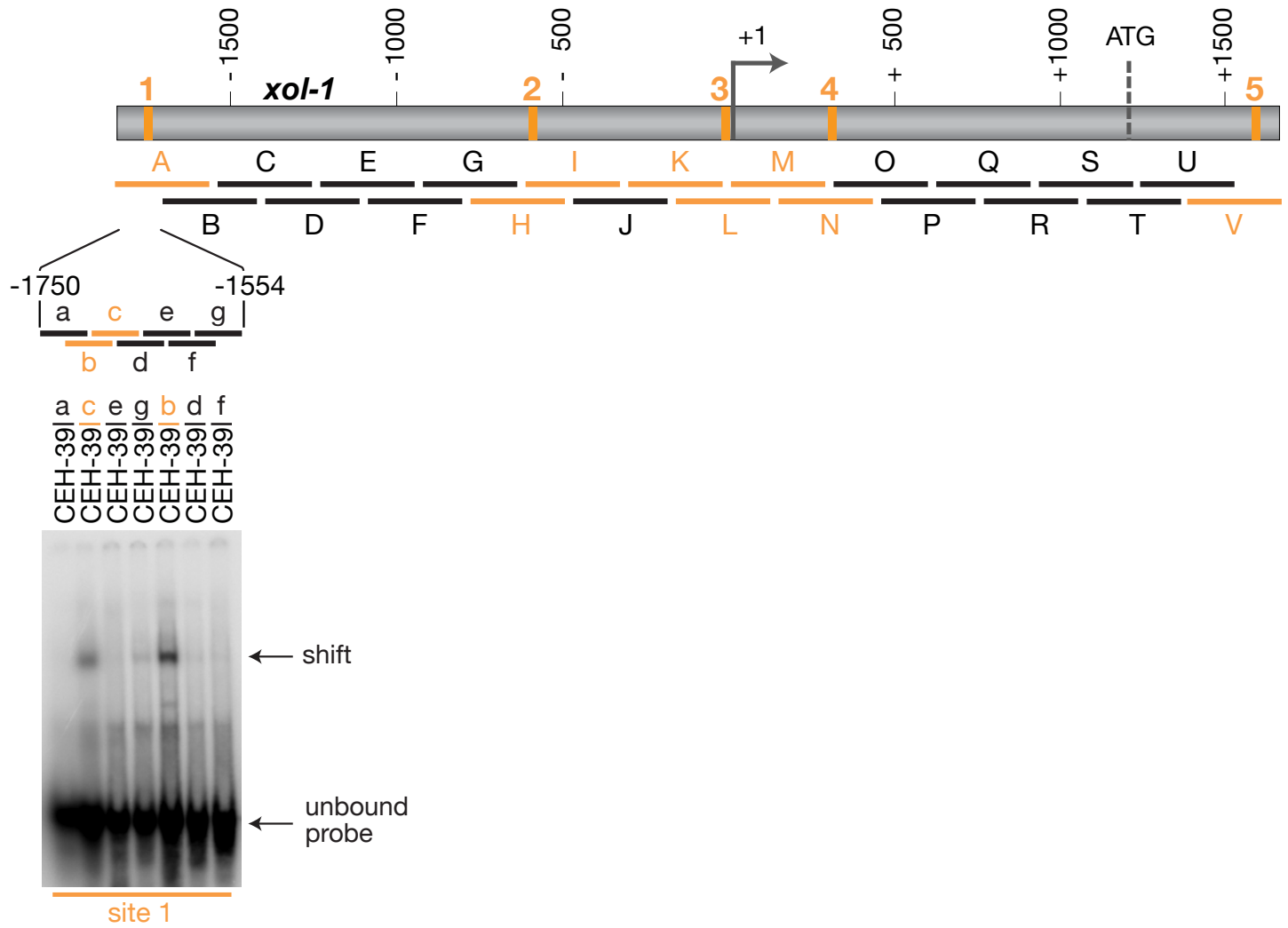


**Supplemental Figure 6. SEX-1 binds directly to multiple sites in *xol-1*.**

(A) *xol-1* schematic for EMSAs using SEX-1 and <sup>32</sup>P-labeled 300 bp DNA fragments (A-V) shows probes positive for SEX-1 binding (J, K, L and P, Q) (red). Positive probes were subdivided into 50 bp overlapping fragments (a-m) and (o-p) that were assessed for SEX-1 binding. The overlapping fragments (a,b), (d,e), (i,j), (k,l) and (o,p) were shifted by the SEX-1 extract but not the non-recombinant nuclear extract (NR); each set contained a single SEX-1 binding site. Shifted fragments of two mobilities were observed, a major species of faster mobility and a minor species of slower mobility. Since the minor band is also supershifted by SEX-1 antibody, it likely contains SEX-1 and reflects the binding of multiple SEX-1 molecules, through a SEX-1 dimerization surface. SEX-1 dimerization is not likely to occur through direct DNA interactions, because mutation of the single NHR response element on the fragment abrogates binding of both shifted species.

(B) Antibody supershift experiments (lanes marked SEX-1 + Ab) for all 5 SEX-1 binding sites established the presence of SEX-1 in the original shifted major and minor bands. For probes containing SEX-1 sites 1 through 5, antibody raised against SEX-1 can supershift (lanes labeled SEX-1+Ab) the slow migrating probe (lanes labeled with SEX-1).

Supplemental Figure 7

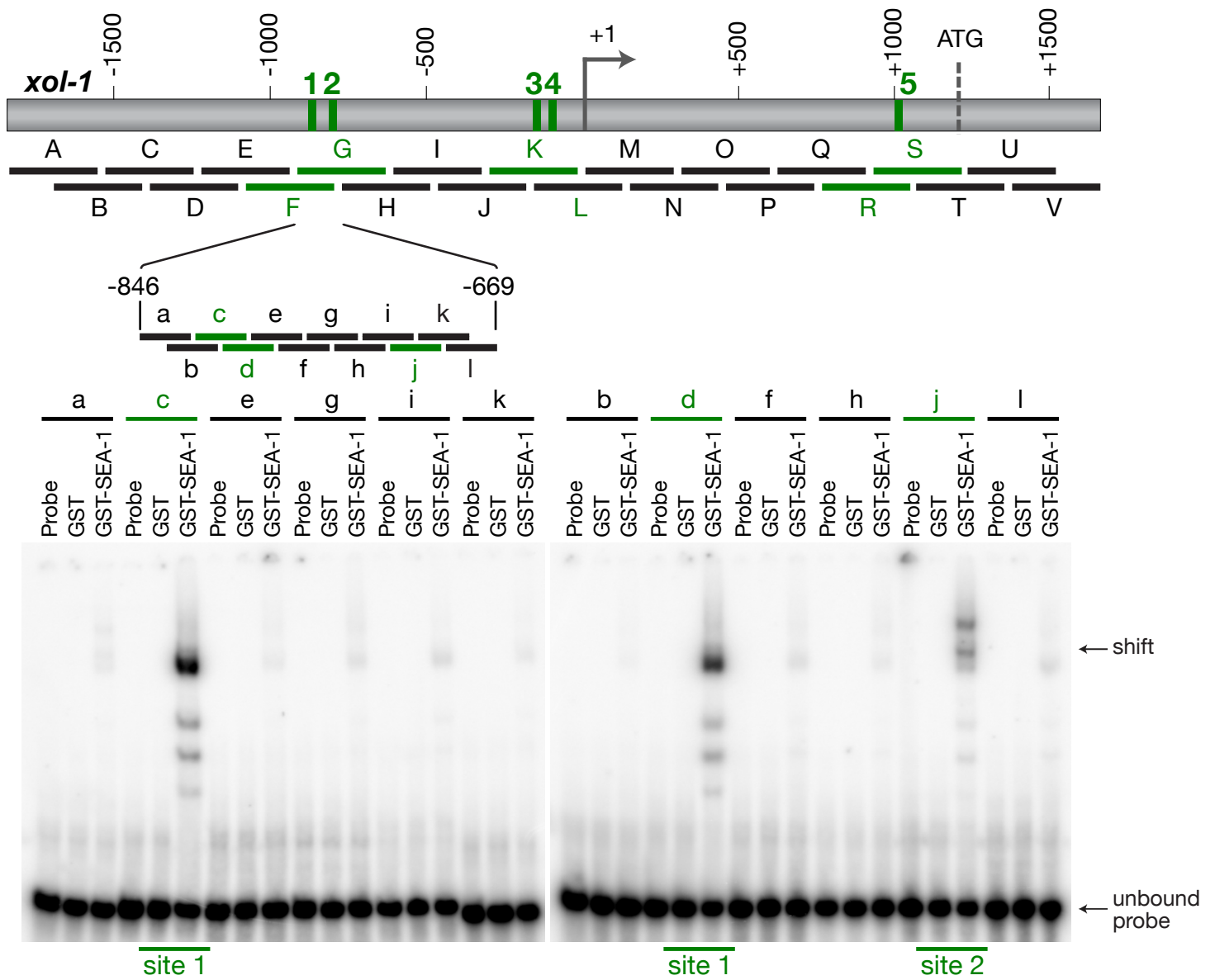


**CEH-39 binds directly to multiple sites in *xol-1*.**

Schematic for EMSAs using CEH-39 and overlapping 300 bp DNA fragments from the *xol-1* promoter and gene. Fragments positive for binding are indicated in orange. Below is the schematic and EMSAs for 50 bp overlapping probes (a-g) used to define the binding site from fragment A. Site 1 is in the overlap between probes b and c.



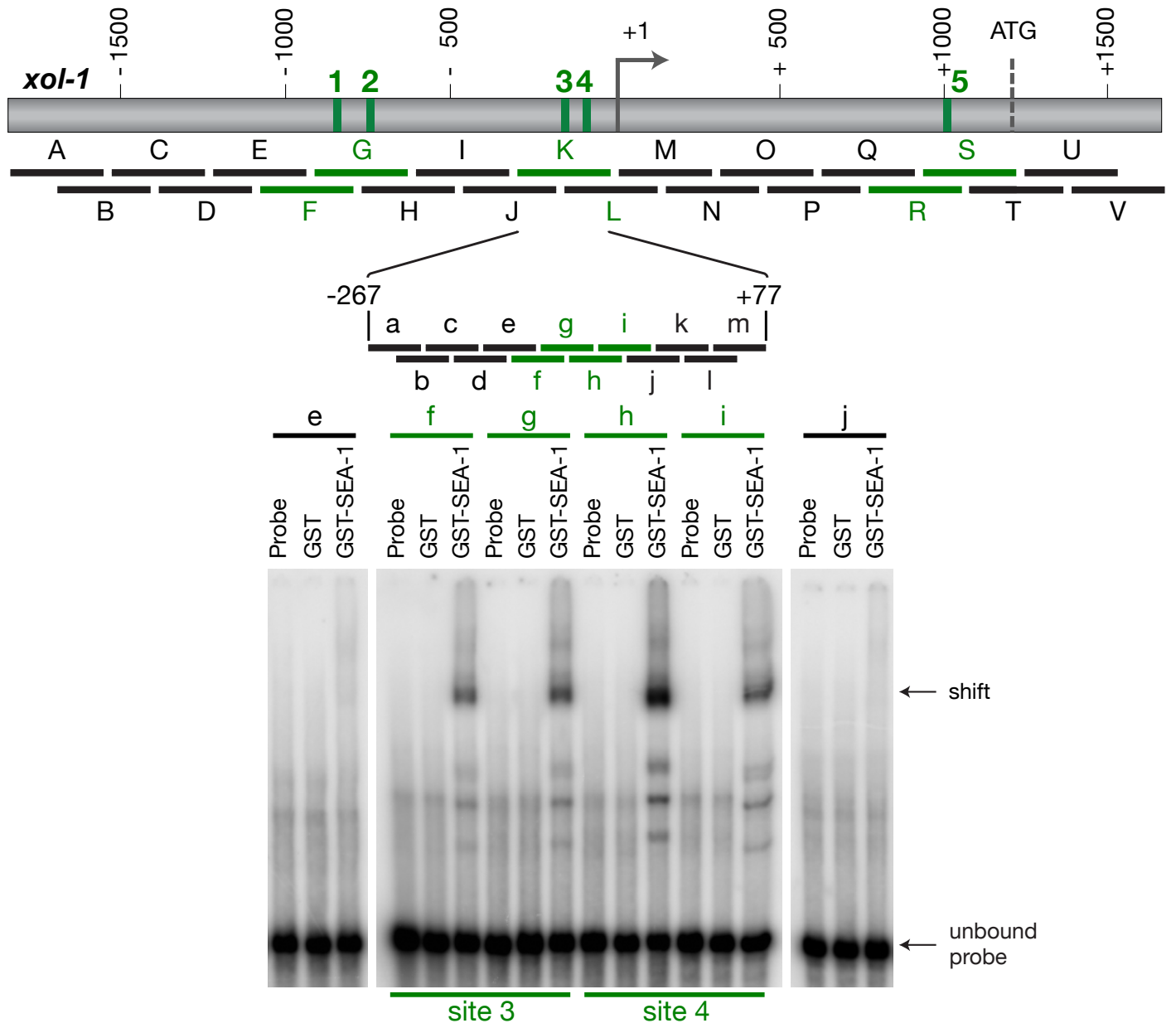
Supplemental Figure 8



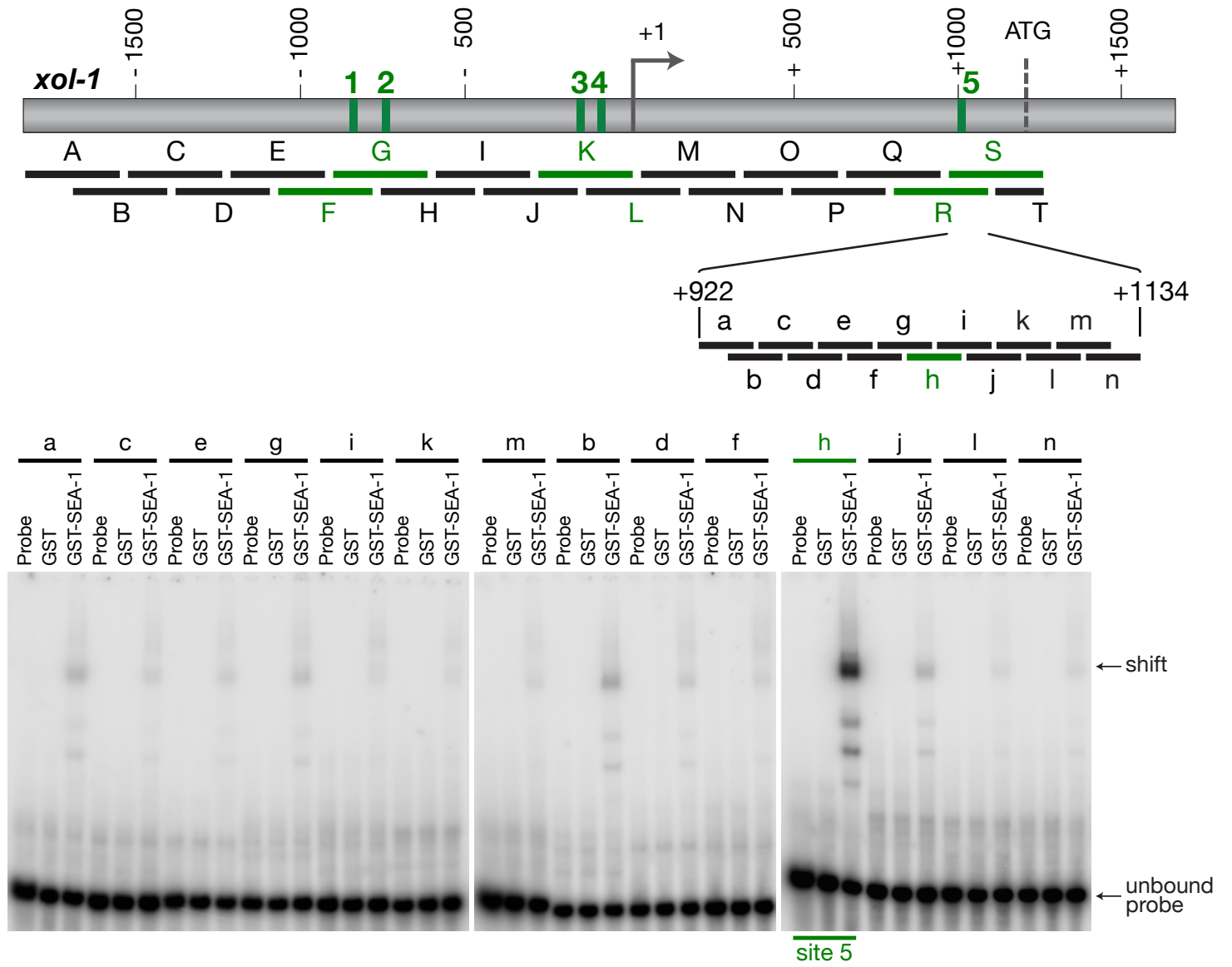
**SEA-1 binds directly to multiple sites in *xol-1*.**

Schematic for the 300 bp DNA fragments in *xol-1* used for EMSAs with SEA-1 shows the location of SEA-1 binding regions (green). Below are the 30 or 50 bp overlapping fragments and EMSAs that yielded the 5 SEA-1 binding sites (green): site 1 (c,d) and site 2 (j) from F-G; site 3 (f,g) and site 4 (h,i) from K; site 5 (h) from R-S. These sites were shifted by GST-SEA-1 but not GST alone.

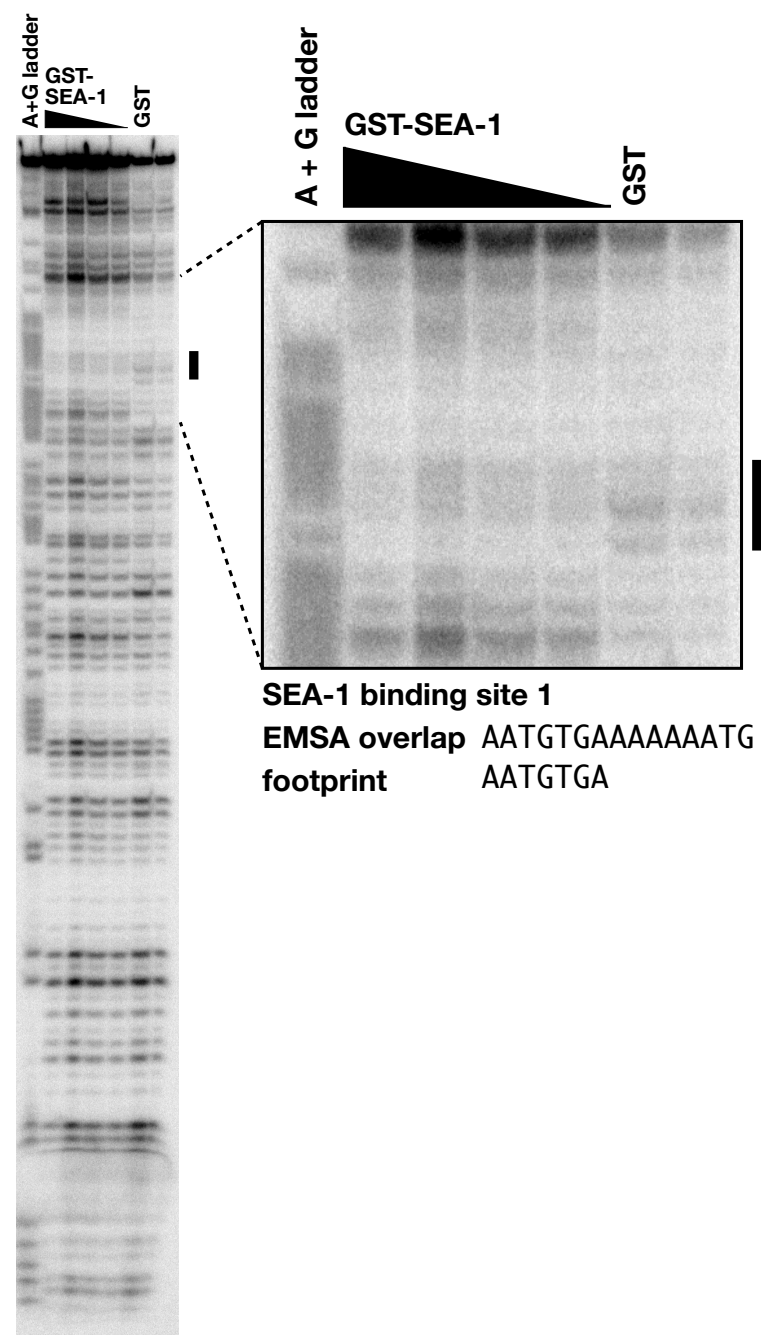
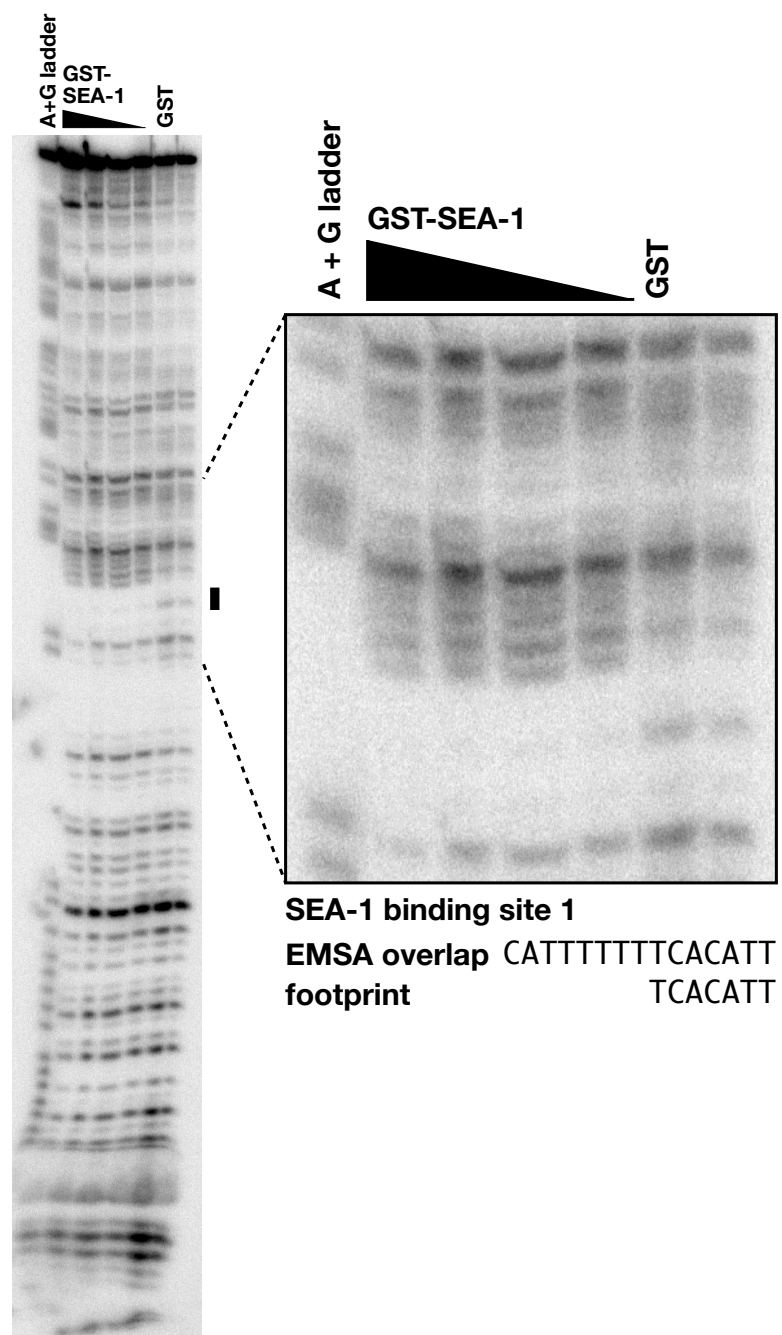
Supplemental Figure 8



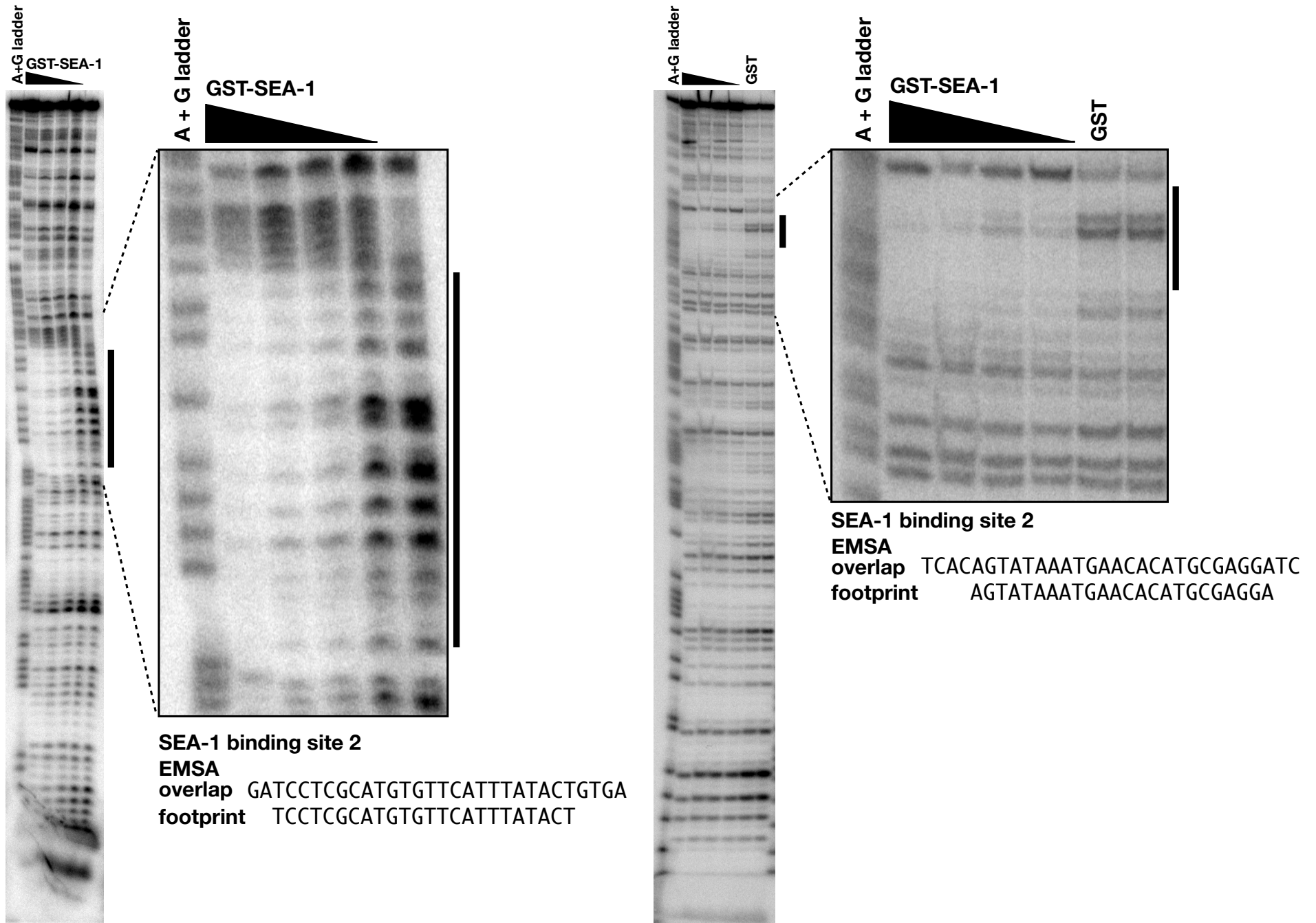
Supplemental Figure 8



Supplemental Figure 9

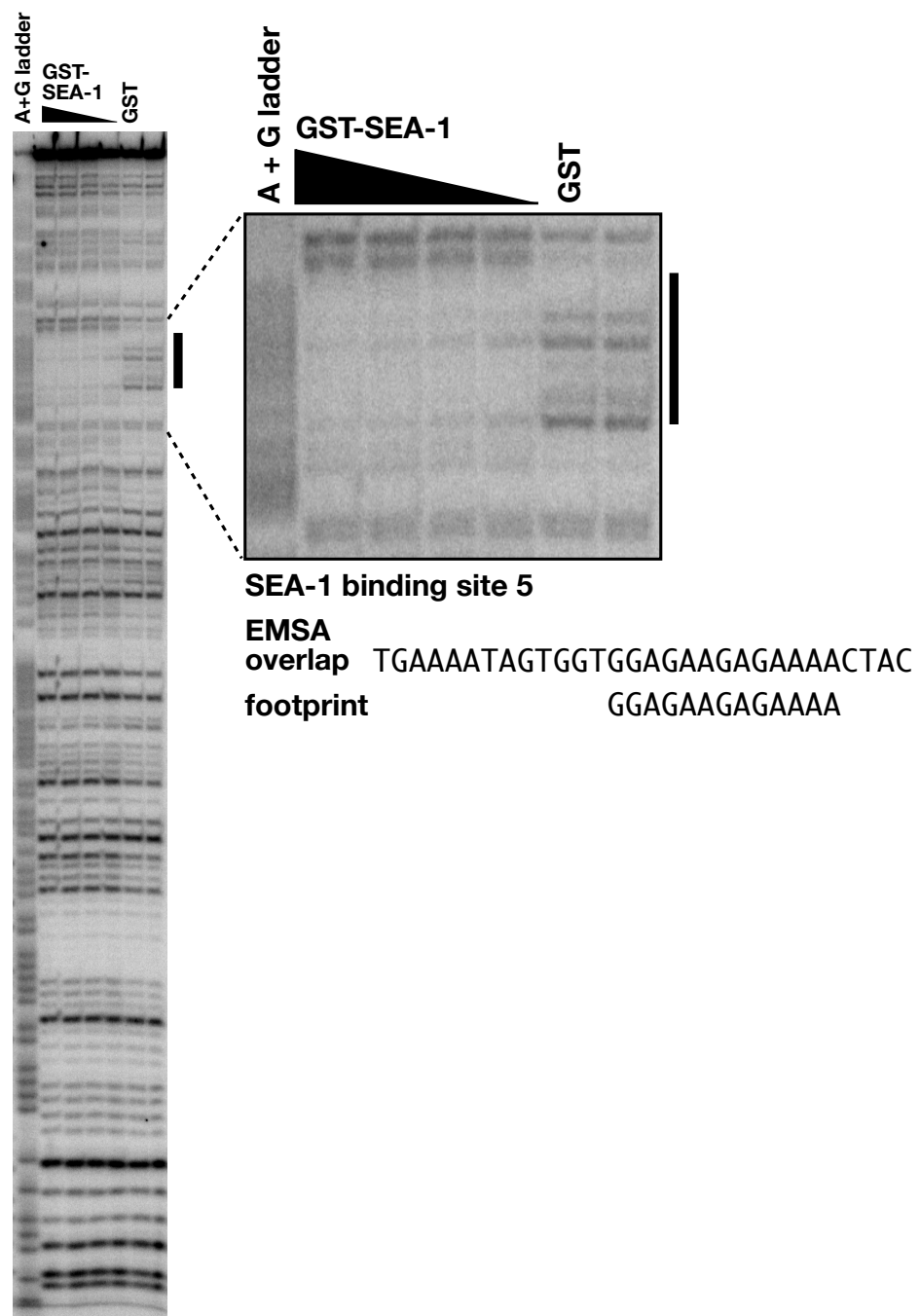
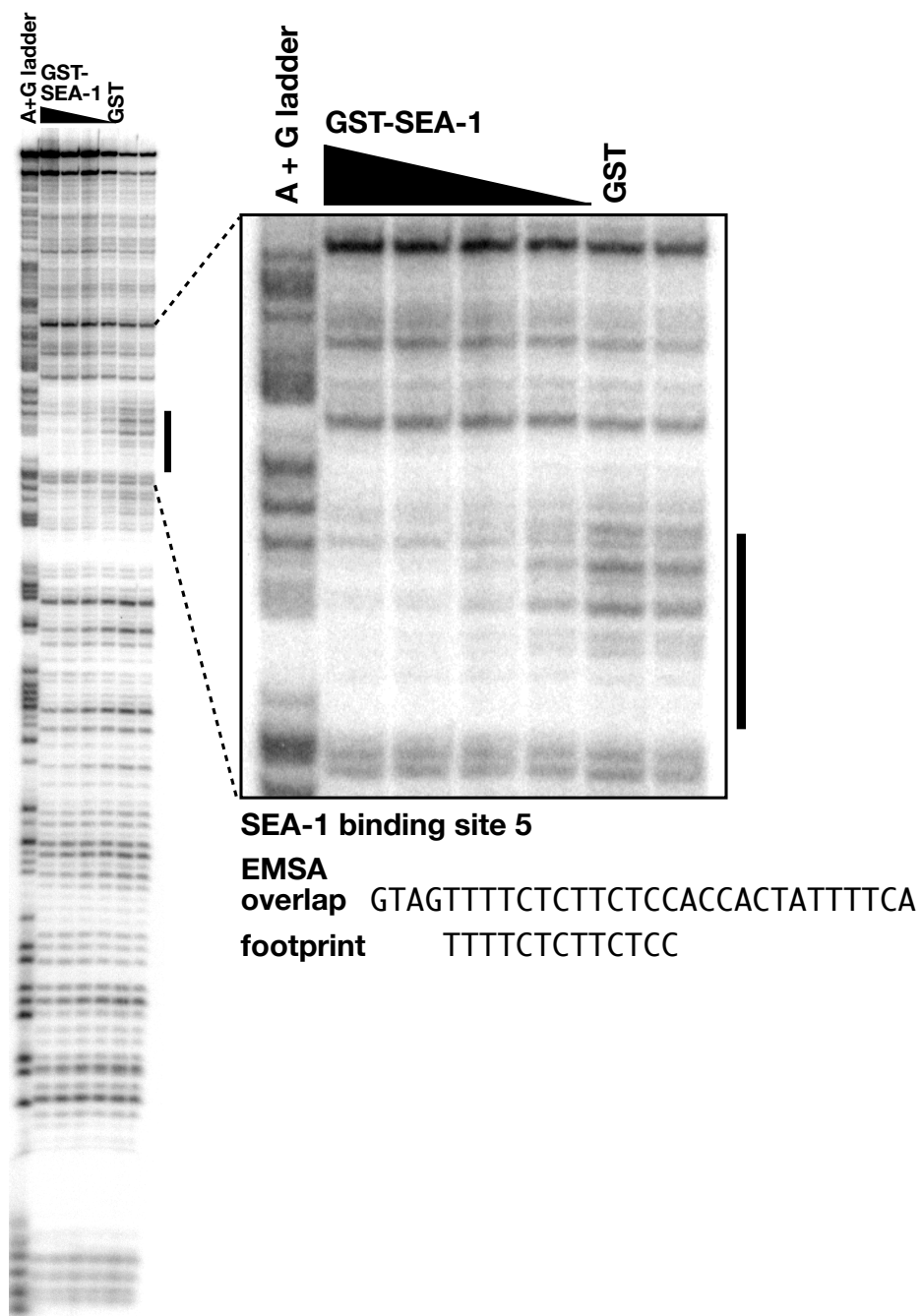


Supplemental Figure 9





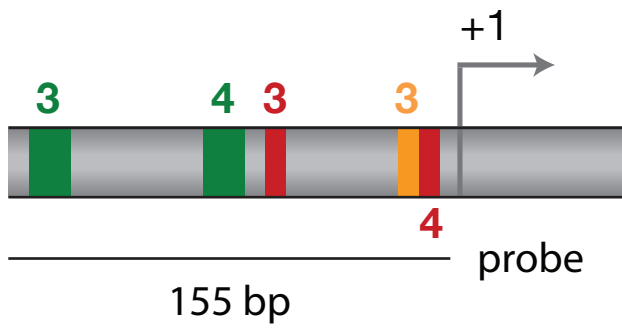
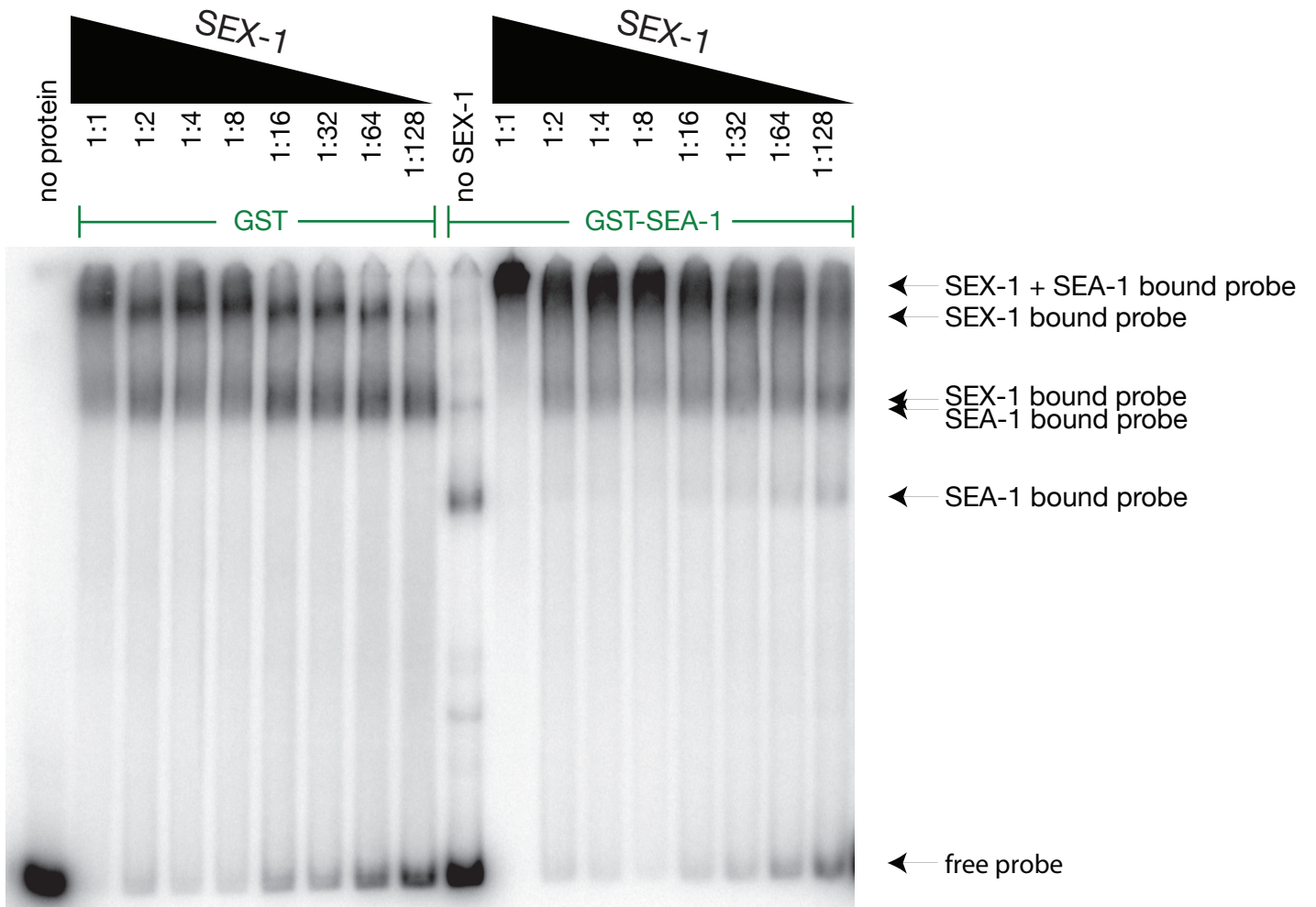
Supplemental Figure 9



**Supplemental Figure 9. DNase I footprinting assays identified five non-canonical T-box binding sites for SEA-1.**

DNase I footprinting assays identify the precise location of SEA-1 binding sites within the binding regions identified by EMSAs. Labeled probes for the forward strand (shown on left) or reverse strand (shown on right) were incubated with either 600 ng of GST as a control, no protein, or a dilution series of 600 ng, 300 ng, 150 ng, and 75 ng GST-SEA-1. The protected region (footprint) (black bar to the right of the gel) is enlarged in an inset to the right of the full-length gel. Each footprinting gel contains a labeled A+G ladder to align and read the protected sequences. Comparison (below the insets) of the SEA-1 protected region in footprint experiments to the sequences in the EMSA probe overlap needed for efficient SEA-1 binding shows that the protected footprints are contained within the EMSA probe overlaps.

Supplemental Figure 10

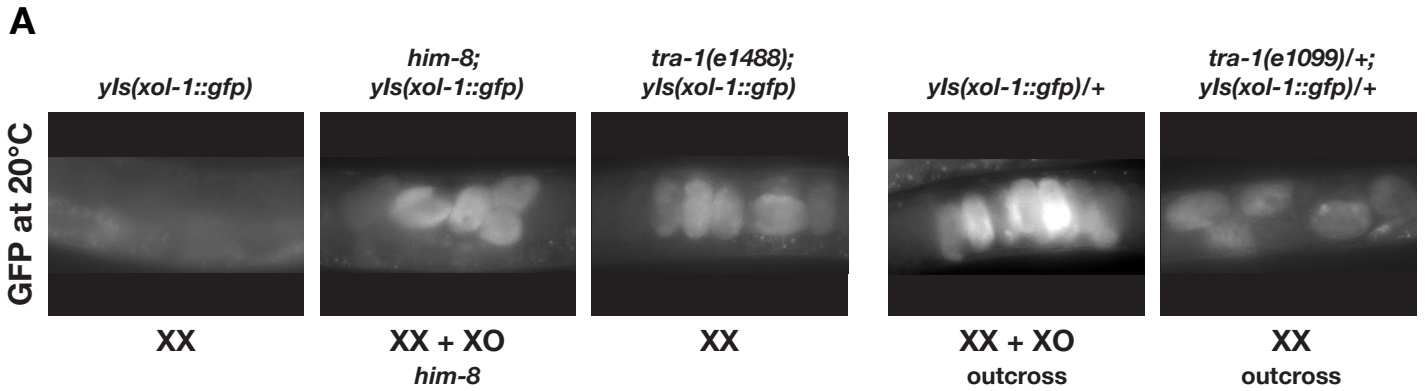




**Supplemental Figure 10. SEX-1 and SEA-1 can co-occupy a fragment of *xol-1* in vitro that contains binding sites for both proteins.**

A 155 bp fragment of *xol-1* that contains two SEX-1 binding sites and two SEA-1 binding sites was labeled and utilized in an EMSA to determine whether binding of SEX-1 interferes with binding of SEA-1 to the same piece of DNA. SEX-1 was titrated in the binding reactions starting at a concentration that can shift all free probe on its own (lane labeled “1:1” dilution on the left half of gel). Two-fold dilutions of SEX-1 were then added in consecutive wells (labeled “1:2”, “1:4”, etc.). With the addition of decreasingly less SEX-1, more probe remained unbound. Separately, a sub-saturating amount of GST-SEA-1 was added to shift less than all free probe (center lane). This constant amount of GST-SEA-1 was then added to each reaction of the SEX-1 titration (right side of gel). Addition of GST-SEA-1 to the reactions with enough SEX-1 to shift all free probe results in a super-shifted protein DNA complex that runs slower than either SEX-1-DNA complexes or SEA-1-DNA complexes, indicating that both SEX-1 and SEA-1 can simultaneously bind the same piece of probe DNA. Reducing the amount of SEX-1 frees up some probe (unbound probe becomes detectable) and the re-emergence of SEX-1-DNA and SEA-1-DNA complexes are detected. This suggests that SEX-1 and SEA-1 co-occupy the same piece of DNA and are unlikely to compete for binding.

## Supplemental Figure 11



**B**

	20°C	25°C
<i>dpy-18; unc-18</i>	91.25	91.32
<i>tra-1(e1099)/dpy-18; unc-18</i>	97.23	96.55
<i>tra-1(e1099); unc-18</i>	90.92	70.41
	n=814	n=1411
<i>dpy-18; unc-18 xol-1</i>	90.80	92.12
<i>tra-1(e1099)/dpy-18; unc-18 xol-1</i>	98.02	97.21
<i>tra-1(e1099); unc-18 xol-1</i>	90.46	90.43
	n=1163	n=521

### Loss of *tra-1* weakly derepress *xol-1* but does not cause significant hermaphrodite lethality at 20°C.

A negative regulatory feedback loop has been proposed to repress *xol-1* by the terminal switch gene in the sex determination regulatory hierarchy, *tra-1* [Hargitai *et al.* (2009) *Development* 136, 3381-3387]. The loop was proposed to function after X:A assessment, perhaps to maintain a low *xol-1* activity state in XX embryos once the major sex determination decision has been made and sexual differentiation is underway. Here we show our investigation of *tra-1*'s influence on *xol-1* repression. We found the contribution to be minimal compared to that of Hargitai *et al.* and interpret our results to mean that the proposed feedback loop does not contribute significantly to *xol-1* repression.

(A) Like Hargitai *et al.*, we found that mutations in *tra-1* weakly derepress a *Pxol-1::gfp* reporter. Gonads of viable animals carrying a *Pxol-1::gfp* transgene, which fuses the first 89 amino acids of XOL-1 onto GFP, were examined using epifluorescence microscopy. *Pxol-1::gfp* reporter activity was low in XX hermaphrodite embryos and was elevated in XO embryos within *him-8* hermaphrodites. The hypomorphic *tra-1(e1488)* XX mutants are intersexual animals with a male body and hermaphrodite gonad and intestine. Self progeny embryos in *tra-1(e1488)* animals showed weak derepression of a *Pxol-1::gfp* reporter, to a level less than that of XO embryos from *him-8* hermaphrodites or a cross. *tra-1(e1099)* is a null allele that causes XX animals to be completely transformed into mating males. *tra-1(e1099) / +* XX embryos from a mating of *tra-1(e1099)* XX males to hermaphrodites carrying an integrated *Pxol-1::gfp* transgene also showed weak derepression of the transgene. The level of GFP fluorescence was considerably lower than that of XO embryos generated by crosses.

### Supplemental Figure 11. (continued)

(B) Even though *tra-1* mutations result in partial derepression of *xol-1*, they do not substantially reduce hermaphrodite viability at 20°C. Although 10% of *tra-1(e1099)* homozygous XX animals were dead under the standard growth condition of 20°C, the lethality was not suppressed by a *xol-1* null mutation, indicating that the lethality was not caused by mis-regulation of *xol-1*. At 25°C, a more extreme growth condition, the lethality increased to 30% and was suppressed in part (to 10% lethality) by the *xol-1* null mutation, indicating that at 25°C part of the lethality is due to *xol-1* mis-regulation. These results are in contrast to those of Hargitai *et al.*, who reported 28% XX lethality at 20°C and 48% at 25°C for a heterozygous *tra-1* null mutant, with 50% suppression of lethality achieved by a *xol-1* null mutation. Hargitai *et al.* compared the XX lethality caused by a heterozygous *tra-1* mutation to the lethality caused by a homozygous *sex-1* mutation using a hypomorphic *sex-1* allele and commented that the *tra-1*-mediated lethality was equivalent to the *sex-1*-mediated lethality. The fair comparison for understanding the relative influence of *tra-1* mutations vs. *sex-1* mutations utilizes the *sex-1(y424)* null, which causes 80% XX lethality in standard growth conditions. The escapers are DPY, slow growing, and produce few progeny, phenotypes reflecting a dosage compensation disruption. In contrast, the *tra-1* escapers are phenotypically wild-type with respect to these dosage compensation phenotypes. A *xol-1* mutation suppresses half of the *sex-1*-induced lethality, and the dosage compensation phenotype of the escapers is strongly suppressed. The effect of *tra-1* mutations is therefore much weaker than the effect of XSE mutations, and a repressive interaction between *tra-1* and *xol-1* is unlikely to constitute a significant feedback loop.

*tra-1(e1099)* XX viability was determined by counting self progeny from *tra-1(e1099)/dpy-18(e364am); unc-18(e81)* hermaphrodites or from *tra-1(e1099)/dpy-18(e364am); unc-18(e81) xol-1(y9)* hermaphrodites. n = number of self progeny

## Supplemental Table 1

Genotype	<i>xol-1</i> copy number	SEM	relative <i>xol-1</i> expression	SEM	relative <i>xol-1</i> expression in <i>sex-1(y424)</i>	SEM
wild-type (no transgene)	2		1		2.8	0.2
<i>xol-1</i> (null) (no transgene)	0.0	0.0	0.0	0.0	0.0	0.0
<i>ceh-39(y414)</i> (no transgene)	2*		1	0.2		
<i>sex-1(y424)</i> (no transgene)	2*		2.8	0.2		
<i>sea-1(y356)</i> (no transgene)	2*		0.9	0.1		
<i>xol-1</i> (null); <i>yIs168[xol-1(+)]</i>	2.1	0.4	1.1	0.1	3.5	0.4
<i>xol-1</i> (null); <i>yIs163[ΔSEA-1 sites]</i>	2.4	0.2	1.5	0.3	2.8	0.4
<i>xol-1</i> (null); <i>yIs167[ΔSEX-1 sites, ΔCEH-39 sites]</i>	2.1	0.2	5.3	0.2	6.9	0.8
<i>xol-1</i> (null); <i>yIs151[xol-1(+)]</i>	10.9	1.1	15.7	1.3	18.3	2.4
<i>xol-1</i> (null); <i>yIs169[ΔCEH-39 sites]</i>	11.3	1.3	18.1	2.1	27.2	3.1

### Mutation of XSE binding sites in a *xol-1* transgene causes increased *xol-1* transcript levels, thereby recapitulating the effect of disrupting XSE genes.

Shown are *xol-1* transcript levels from the endogenous *xol-1* locus or from *xol-1* transgenes carrying either a wild-type or mutant regulatory region deficient in XSE or ASE binding sites. *xol-1* transcripts from transgenes were assessed by qPCR in mixed stage XX embryos carrying a homozygous deletion of the endogenous *xol-1* gene and were compared to those from the endogenous *xol-1* gene of wild-type XX embryos. *xol-1* gene copy number was determined for each homozygous transgene strain using qPCR and was standardized to genomic *xol-1* copy number in wild-type XX animals. Comparisons of *xol-1* transcript levels were made between transgenic lines with equivalent *xol-1* copy numbers. SEM, standard error of the mean. *xol-1* copy number for genotypes marked with an asterisk were inferred to be 2. For both *xol-1* copy number and *xol-1* transcript determination, all samples were grown in triplicate and prepared separately from each independent culture. To assess the effect of disrupting *sex-1* on *xol-1* expression, transgenes were crossed into a *sex-1(y424)* strain.

Since multiple copies of *xol-1* or removal of repressor binding sites in *xol-1* can cause *xol-1* overexpression and hermaphrodite lethality, transgenic strains were maintained on *xol-1* feeding RNAi. To determine *xol-1* expression levels, animals were removed from feeding RNAi and transferred to standard NGM plates with OP50 bacteria and grown for two generations prior to extracting RNA. Animals that had a single copy *xol-1* transgene that lacked CEH-39 and SEX-1 binding sites produced dead embryos after two generations on standard plates. Similarly, strains that possessed several copies of the *xol-1* transgene also produced dead embryos two generations removed from the rescuing effects of *xol-1* feeding RNAi. Therefore, the assayed embryo population contained dead embryos.

## Supplemental Materials and Methods

### *Isolation of sea-2 alleles*

To obtain a *sea-2* null allele, *Mos1* was excised from the germline of *y407* mutants. First, *y407*; *yEx660* animals were generated and heat shocked as described above to mobilize *Mos1*. All 96 F1 progeny that had lost the array after heat shock were cloned, and 15 F2 progeny were collected from each of the 96 clones and placed onto new plates. After 24 hr, individual pools of F2 progeny were analyzed by PCR with primers flanking the insertion site (5' GCCCGATGAGCTGATGACGTTAGATCCG 3', 5' CGACGAAGCGATCGTTCGGATGATACC 3'). Of 96 F1 progeny, 5 produced a shorter PCR product. Sixty F3 were cloned from each of the 5 F2 pools and re-analyzed in the next generation to identify clones with a *Mos1* excision event. Three independent excision events were detected, and the *y426* allele had the most useful lesion: 5 bp of *Mos1* left in exon 4. The *sea-2* sequence in *y426* included GCTGTTTTTAccataCGTGAGTTGT, where capitalized letters represent *sea-2* sequence and lower case letters represent inserted *Mos1* sequence.

A separate *sea-2* deletion allele, *y410*, was isolated by screening our frozen *C. elegans* deletion library using the poison primer method (Edgley et al. 2002). Primer sequences are available upon request. Homozygous *y410* animals were isolated and backcrossed four times. *y410* is a 735 bp deletion of K10G6.3 that eliminates nucleotides 380 to 1114, relative to the first SL1 leader sequence splice site. This eliminates some of intron 1 and extends through most of exon 3 and is predicted to cause a frameshift leading to an early stop.

### *RNA interference*

RNAi of *sea-2* and other ORFs identified in the transposon screen was achieved by injecting dsRNA (1-4 µg/µl) to the corresponding gene into *fox-1 sex-1*; *yEx660* hermaphrodites. The

number of viable *gfp(+)* and *gfp(-)* XX adults were counted and percent viability was calculated as the (number of *gfp(-)* adults)/(total adults counted) X 100. *sdc-2* RNAi was performed by feeding as described (Kamath et al. 2003).

#### *Rescue of sea-2 and analysis of sea-2 transcript*

Rescue of *sea-2* was obtained by injecting wild-type animals with a DNA mixture of cosmid K10G6 (10 ng/μl), pPD97/98 (*unc-122::gfp*; 30 ng/μl), and pBlueScript (60 ng/μl) to generate the extrachromosomal array *yEx688*. *yEx688* males were crossed to *sea-2(y407)* hermaphrodites to generate the strain *y407; yEx688*. Heterozygous *y407/+; yEx688* males were then crossed to *y407; fox-1 sex-1* hermaphrodites and the resulting *gfp(+)* male cross progeny crossed back to *y407; fox-1 sex-1* hermaphrodites. A total of 189 *gfp(+)* males and 21 *gfp(+)* hermaphrodites were scored from several crosses. 15 of 21 hermaphrodites were sterile and/or died, while 6 of 21 were fertile but did not produce any *gfp(+)* progeny. A chromosomal integration of *yEx688* was obtained after UV treatment in a Stratalinker at 27.5 mJ/cm<sup>2</sup> (Mitani 1995).

Sequence of *sea-2* transcripts was obtained by reverse transcription of wild-type RNA followed by PCR amplification of fragments, gel purification, and sequence analysis. The 5' *trans*-spliced sequence was obtained by PCR amplification with an SL1 primer (GGTTTAATTACCCAAGTTTG) and a gene-specific primer.

Quantitative real-time PCR analysis of *sea-2* transcript levels was performed on three independent cDNA preparations from embryos according to the protocol in Gladden and Meyer, 2007. *sea-2* transcript levels were normalized to *nhr-64* transcript levels.

### *Mapping the start site of xol-1 transcription using RT-PCR*

RT-PCR assay was performed as previously described (Morton and Blumenthal 2011). Young embryos (embryos with less than 20 nuclei on average) were harvested by bleaching and RNA was isolated with TRIzol reagent (Invitrogen) and digested with RQ1 RNase-free, DNase (Promega). cDNAs were generated from 5 mg of total RNA using the ProtoScript First Strand cDNA Synthesis Kit (New England Biolabs). Gene specific primers were synthesized (sequences available upon request), PCR performed, and resulting PCR products resolved by gel electrophoresis on a 2% agarose/1X TAE gel.

### *Analysis of tra-1's role in xol-1 regulation*

Fluorescence microscopy of *xol-1::gfp* was performed on anesthetized adult animals of the indicated genotype. Since *tra-1(e1099)* animals are fully transformed mating males, cross progeny embryos were examined by crossing *tra-1(e1099)* males into *yIs(xol-1::gfp)* hermaphrodites.

*tra-1(e1099)* viability was determined by counting the resulting offspring from either *tra-1(e1099) / dpy-18(e364am)* III; *unc-18(e81)* XX or *tra-1(e1099)* III / *dpy-18(e364am)*; *unc-18(e81).xol-1(y9)* XX parents. Viability was determined from animals maintained at 20°C and 25°C.

### *Generation and analysis of xol-1 transgenes*

Mutations in XSE and ASE binding sites were generated in pLM9, a vector containing *xol-1* promoter, gene, and 3' UTR sequence. The first three bases of each SEX-1 hexanucleotide binding site was mutated to TTT, while all six bases of each of CEH-39 binding sites were mutated to GGGGGG using Phusion polymerase mediated mutagenesis (Finnzymes).

The first SEA-1 binding site was mutated from TTTCACA to GGGGGGG using Phusion polymerase mediated mutagenesis (Finnzymes). The sequence of the remaining four SEA-1 binding sites were scrambled using SDSC Biology WorkBench (<http://workbench.sdsc.edu/>) and introduced into pLM9 using standard splice-by-overlap-extension PCR. SEA-1 binding were mutated as follows:

Binding site 1 TTTCACA mutated to GGGGGGG.

Binding site 2: GATCCTCGCATGTGTTTCATTTATACTGTGA mutated to GGCGTATCACCGCGATTTATTTTGCTTATA.

Binding site 3: TCATCTTCTCTTCTTCTTGCCTCT mutated to TTTTCCTCCTCCCCTTATTTTTCG.

Binding site 4: ATGACAACCTGCGCTCTATCGCCAC mutated to ACTGACTCAGAACCTTCGCCCATG.

Binding site 5: GTAGTTTTCTCTTCTCCACCACTATTTTCA mutated to GTACATTTTCTCGTACTATCTCCATCTTC.

Wild type and mutant *xol-1* genes (encompassing 1923 bp 5' of the *xol-1* TSS, 1203 bp of the *xol-1* outtron, the *xol-1* ORF, and 694 bp 3' of the ORF) were excised from pLM9 and cloned into pER717.1 (a biolistic targeting vector encoding two selectable markers: pharyngeal specific GFP and UNC-119). 20-30 µg of pER717.1 was used to coat 50 µg of 1 µm gold beads (BioRad) and bombardment of *unc-119(ed3)* worms were performed as described (Praitis et al. 2001).

#### *Analysis of xol-1 transgene copy number*

N2 genomic DNA was isolated as follows. Worms that had been grown on NGM agarose plates until the bacterial OP50 lawn was cleared were washed extensively in M9 media, and the



resulting worm pellet was frozen in liquid nitrogen. The pellet was thawed and then resuspended in an equal volume of extraction buffer (10 mM Tris-Cl pH 8, 1mM EDTA, 100 mM NaCl, 1% SDS, and 0.2 µg/ml proteinase K). The sample was incubated at 50°C with rocking for 1 hr, supplemented to 0.4 µg/ml proteinase K, and incubated for another hr. The lysate was then phenol extracted, phenol/chloroform/isoamyl alcohol extracted, and chloroform extracted. The DNA was precipitated by addition of NaOAc pH 6 to a final concentration of 0.3 M with 2.5 X the volume of 100%, room temperature ethanol, then washed in 70% ethanol, and re-dissolved in 10 mM Tris-Cl pH 8. Contaminating RNA was digested with 20 µg of RNase A at 37°C for 1 hr and the remaining genomic DNA was then re-extracted, precipitated, and re-dissolved as described above.

Genomic DNA was then used to generate a standard curve for *xol-1* copy number using the equivalent mass of DNA to yield approximately  $5 \times 10^5$ ,  $5 \times 10^4$ ,  $5 \times 10^3$ ,  $5 \times 10^2$ , and  $5 \times 10^1$  genomes per qPCR reaction. The standard curve was validated using the *xol-1* plasmid pLM9 as a control. Transgene copy number was normalized to genomic N2 copy number. For each genotype, DNA samples were prepared in triplicate from independently grown cultures. PCR was performed on a DNA Engine Opticon 2 Real-Time Cycler (MJ Research) using the following cycle conditions: After an initial incubation at 95°C for 5 min, 40 cycles of (94°C for 30 sec, 60°C for 30 sec, 72°C for 1 min, 78°C for 10 sec, followed by fluorescence scan) were executed.

Comparisons of *xol-1* transcript levels using qPCR were made among transgenic lines with similar *xol-1* copy numbers. Transgenic lines were removed from *xol-1* RNAi feeding plates two generations prior to RNA isolation. To prepare RNA, mixed stage embryos were isolated from asynchronously grown hermaphrodites on NGM plates with OP50 bacterial lawns. RNA

was isolated with TRIzol reagent (Invitrogen) and digested with RQ1 RNase-free, DNase (Promega). cDNAs were generated from 5 mg of total RNA using the ProtoScript First Strand cDNA Synthesis Kit (New England Biolabs). qPCR analysis was performed as described, using the  $2^{-\Delta\Delta CT}$  to quantify relative transcript abundance (Livak and Schmittgen 2001; Gladden and Meyer 2007). The reference transcript was the *fasn-1* fatty acid synthase gene transcript (ORF: F32H2.5), which is made constitutively throughout embryogenesis. Samples were prepared in triplicate from independently grown cultures.

## References

- Edgley M, D'Souza A, Moulder G, McKay S, Shen B, Gilchrist E, Moerman D, Barstead R. 2002. Improved detection of small deletions in complex pools of DNA. *Nucleic Acids Res* **30**: e52.
- Gladden JM, Meyer BJ. 2007. A ONECUT homeodomain protein communicates X chromosome dose to specify *Caenorhabditis elegans* sexual fate by repressing a sex switch gene. *Genetics* **177**: 1621-1637.
- Kamath RS, Fraser AG, Dong Y, Poulin G, Durbin R, Gotta M, Kanapin A, Le Bot N, Moreno S, Sohrmann M et al. 2003. Systematic functional analysis of the *Caenorhabditis elegans* genome using RNAi. *Nature* **421**: 231-237.
- Livak KJ, Schmittgen TD. 2001. Analysis of relative gene expression data using real-time quantitative PCR and the  $2^{-(\Delta\Delta C(T))}$  Method. *Methods* **25**: 402-408.
- Mitani S. 1995. Genetic regulation of *mec-3* gene expression implicated in the specification of the mechanosensory neuron cell types in *Caenorhabditis elegans*. *Develop Growth Differ* **37**: 551-557.
- Morton JJ, Blumenthal T. 2011. Identification of transcription start sites of trans-spliced genes: uncovering unusual operon arrangements. *RNA* **17**: 327-337.
- Praitis V, Casey E, Collar D, Austin J. 2001. Creation of low-copy integrated transgenic lines in *Caenorhabditis elegans*. *Genetics* **157**: 1217-1226.